Supporting Information for *Topographic roughness on forested hillslopes: a theoretical approach for quantifying hillslope sediment flux from tree throw*

Tyler H. Doane[1], Douglas A. Edmonds[1], Brian J. Yanites[1], Quinn W. Lewis [2]

[1]Indiana University-Bloomington, Bloomington, IN, USA

[2]Waterloo University, Waterloo, ON, Canada

Tyler H. Doane[doanet@iu.edu]

Contents of this file

1. Text S1 to S4

2. Figures S1 to S4

3. Tables S1

Introduction Here we provide supplemental information that supports the results presented in the main text. We address several items. First, we consider the role that DEM resolution plays. We compare measurements of topographic variance of the same hillslope from two different data sources and demonstrate that, so long as a DEM has a resolution less than a meter that it captures the majority of topographic variance. Second, we demonstrate that different flux models do not result in a meaningful difference in the

———

June 23, 2021, 8:04pm

evolution of topographic variance of a single pit-mound couplet. Therefore, the results do not strongly depend on the choice of flux model. Third, we explain how we parameterized natural pit-mound couplets using high resolution topographic data. Fourth, we consider how initial pit-mound couplet geometry will vary on increasingly sloped terrain. On steeper slopes, more sediment is 'thrown' downslope and l increases. We present results from a simple numerical exercise which demonstrates that l increases linearly with land-surface slope. Last, we present a table of measured R values for 8 directions and the number of measurements in each direction.

1. Resolution We note that the measured topographic variance may differ between the 0.76 m and 0.25m resolution datasets. We anticipate that the finer resolution is closer to the actual resolution, however, we also anticipate that the difference between them is relatively small and does not alter the quantification of tree throw. To demonstrate this, measurements of topographic variance of a single hillslope on private property in Washington County demonstrates similar estimates of the topographic variance whether it is calculated using 0.25 m or 0.76 m-resolution topographic data. On a single hillslope, the measured topographic variance on 0.76 m and 0.25 m resolution topographic data are 0.012 and 0.014 m^2. We are confident that the 0.76 m resolution data is capable of capturing a clear majority of the topographic variance at the meter scale. Lidar data for the high resolution DEM from Washington County was collected by a drone in December 2018. Data collection and processing are outlined in (Lewis et al., 2020).

2. Flux Models We have developed and demonstrated a theory for topographic roughness of forest floors that casts the expected topographic roughness in terms of the rate of

tree throw production and the rate of topographic degradation by linear diffusion which is driven by creep-like processes. There are alternatives to linear diffusion to describe topographic evolution, namely nonlinear (Roering et al., 2001, 2007) and soil thickness (Furbish et al., 2009; Mudd & Furbish, 2004) dependent models. The nonlinear model (CITE Roering et al., 1999) is widely used and states that the flux increases nonlinearly with land-surface slope until a critical gradient,

$$q_c = -D_{cn}\frac{\nabla\zeta}{1 - \left(\frac{|\nabla\zeta|}{S_c}\right)^2} \,, \tag{1}$$

where D_n $[\text{L}^2 \ \text{T}^{-1}]$ is a topographic diffusivity and S_c is a critical slope above which the flux is unbound. A soil thickness-dependent model results from variations in particle motions that vary with depth within the soil. In most soils, porosity decreases with depth and leads to an exponential-like porosity profile which results in an exponential particle velocity profile. In general, thicker soils will have a greater particle velocity near the surface and have larger depth-averaged velocities which leads to a soil-thickness dependency which can be approximated by (Furbish et al., 2009),

$$q_c = -D_n h(x)\frac{\partial\zeta}{\partial x} \,, \tag{2}$$

where D_{ch} $[\text{L} \ \text{T}^{-1}]$ is another topographic diffusivity for creep-like processes but has different units than D_c and incorporates the depth-dependency of transport. Using either of these two alternatives to describe the flux will change the time evolution of pit-mound couplets. Numerical simulation of pit-mound couplets according to all three models demonstrates that, although they lead to slight differences in topographic evolution, the evolution of topographic variance follow similar paths.

3. Fitting Pit-Mound Couplets

We use high resolution DEMs with 0.25 m resolution to inform our parameters for pit-mound couplet geometry. An approximately 1 km^2 plot of land in south-central Indiana was scanned with a lidar-equipped UAV-drone. This particular site has over 600 mapped pit-mound couplets. We selected over 100 of these and fit the idealized geometry to them using a routine in Python which returned values for A, l, w, the orientation, and a squared difference between the observed and modeled. The average difference between observed and modeled is often less than 0.1 meters (Figure B1). In many cases, the amplitudes and dimensions of the couplets appear to match the natural couplets. However, the mismatch also includes the differences between the rough and potentially sloped ground outside of the couplet which contributes to the mismatch values.

4. Initial Pit-Mound Geometry We expect that the initial pit-mound couplet geometry varies with slope because, on steeper slopes, more sediment is deposited downslope of the pit. This will lengthen the couplet, and l should be longer on steeper slopes. We have created a simple one-dimensional model that simulates the initial uprooting and deposition of sediment on hillslopes with different steepness. The model treats a root mass as a one-dimensional rectangle that gets uprooted so that the long axis is perpendicular to the land-surface. This mass of sediment is then virtually dropped to the land-surface which creates an angular profile of a pit-mound couplet, which has unrealistic slopes (Figure S4a). The model numerically diffuses the angular pit-mound couplet until the maximum slope is below a critical slope. In this case, we have set a critical slope of 1. Running this model on couplets formed on different slopes produces pit-mount couplet geometries that vary with land-surface slope (Figure S4b). In particular, there is a nonlinear relation-

ship between the length-scale of couplet geometries and land-surface slope (Figure S4c). We simplify this relationship and assume a linear relationship as most slopes in southern Indiana are below 0.6.

Data Table of measured R values by direction and the number of hillslopes measured.

| Aspect	$\bar{R}$	# hillslopes
North	0.18	292
Northeast	0.22	410
East	0.22	463
Southeast	0.19	189
South	0.19	63
Southwest	0.16	100
West	0.14	163
Northwest	0.17	231

References

Furbish, D. J., Haff, P. K., Dietrich, W. E., & Heimsath, A. M. (2009). Statistical description of slope-dependent soil transport and the diffusion-like coefficient. *Journal of Geophysical Research*, *114*, F00A05. doi: 10.1029/2009JF001267

Lewis, Q. W., Edmonds, D. A., & Yanites, B. J. (2020). Integrated uas and lidar reveals the importance of land cover and flood magnitude on the formation of incipient chute holes and chute cutoff development. *Earth Surface Processes and Landforms*, *45*(6), 1441–1455.

Mudd, S. M., & Furbish, D. J. (2004). Influence of chemical denudation on hillslope morphology: INFLUENCE OF CHEMICAL DENUDATION ON HILLSLOPES. *Journal of Geophysical Research: Earth Surface*, *109*(F2). doi: 10.1029/2003JF000087

Roering, J. J., Kirchner, J. W., & Dietrich, W. E. (2001). Hillslope evolution by nonlinear,

slope-dependent transport: Steady state morphology and equilibrium adjustment timescales. *Journal of Geophysical Research: Solid Earth*, *106*(B8), 16499–16513. doi: 10.1029/2001JB000323

Roering, J. J., Perron, J. T., & Kirchner, J. W. (2007). Functional relationships between denudation and hillslope form and relief. *Earth and Planetary Science Letters*, *264*(1-2), 245–258. doi: 10.1016/j.epsl.2007.09.035
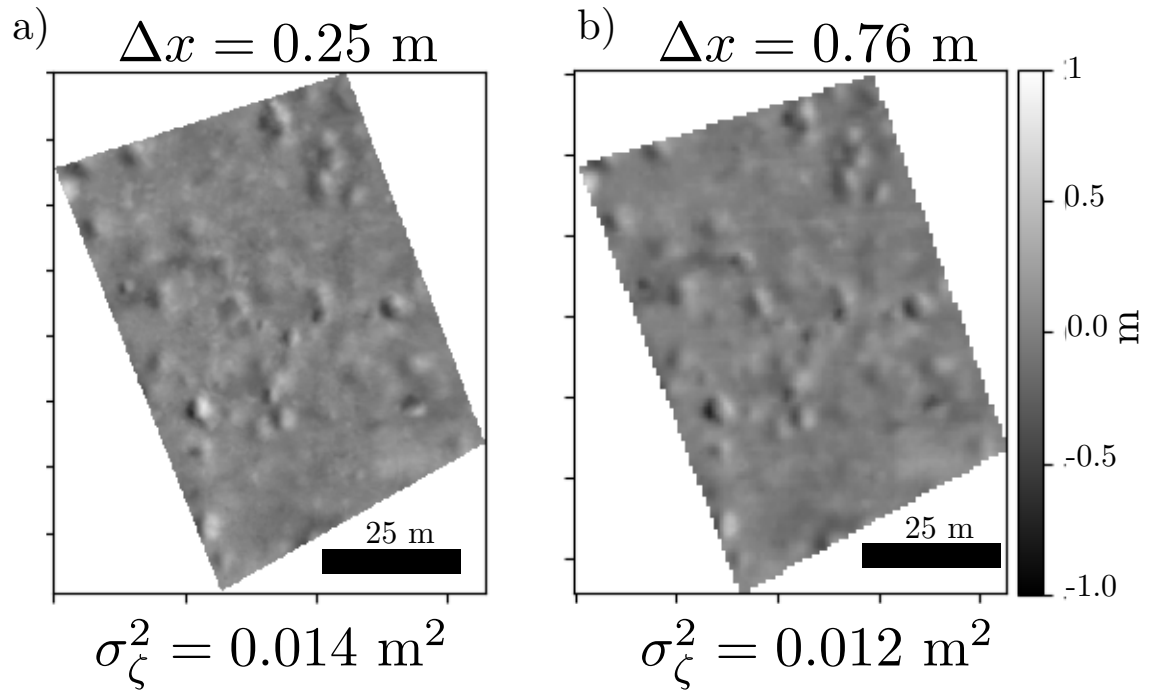
Figure S1. High pass filter of topography of a hillslope in Washington County, IN from 0.25-m (a) and 0.76-m (b) resolution data. The same pit-mound couplets are clearly visible in both datasets and measured variance values are similar.
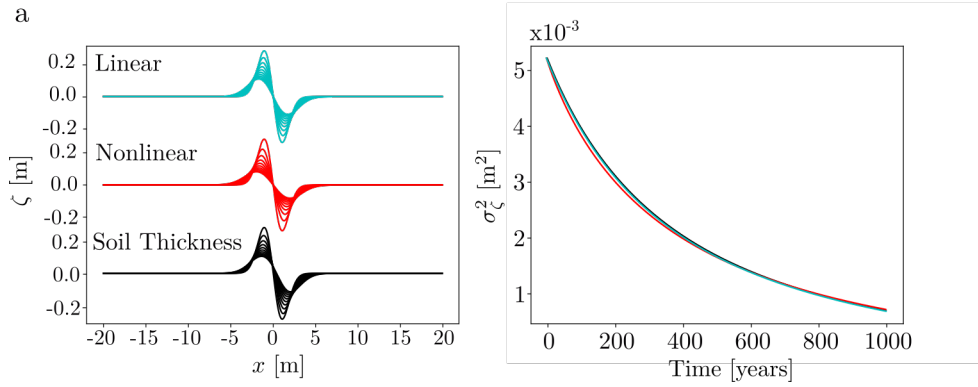
Figure S2. (a) Topographic evolution of a pit-mound couplet according to linear, non-linear, and soil thickness-dependent transport models. Pit-mound couplets were originally on a background slope of 0.4 and we have used S_c=1.2 and μ_h=1 m (b) Time evolution of topographic variance of pit mound couplets according to all three models. The choice of model is apparently relatively unimportant for the time-series of topographic variance of pit-mound couplets.
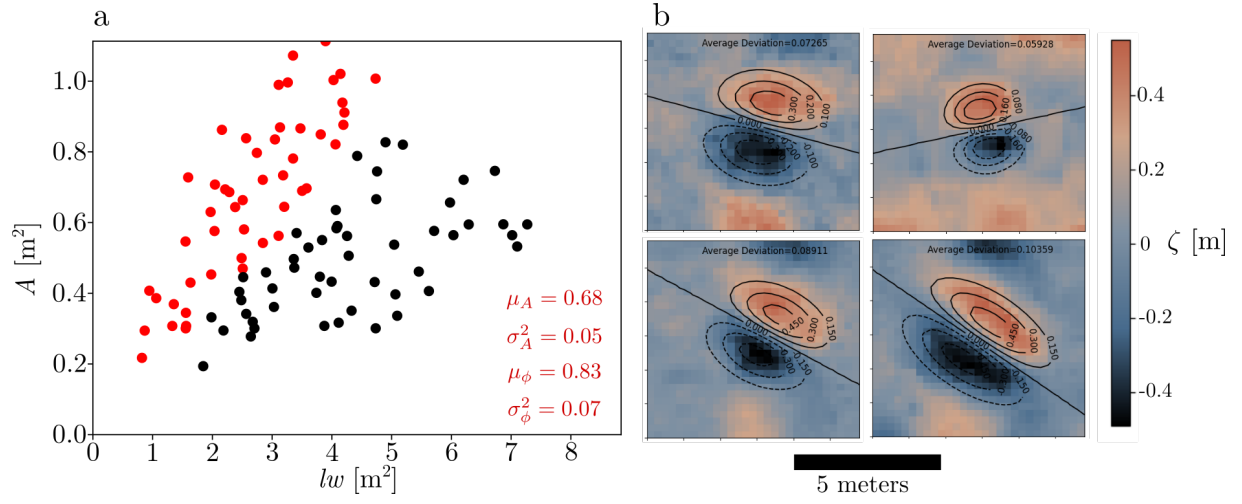
Figure S3. (a) Parameters extracted from 101 couplets from 0.25 m resolution lidar. Red dots are identified as the freshest as the 50 highest values of A/lw. (b) Four examples of natural couplets (colored surface) and the fit couplet (contours) with average deviation over the domain recorded in the top of the image.
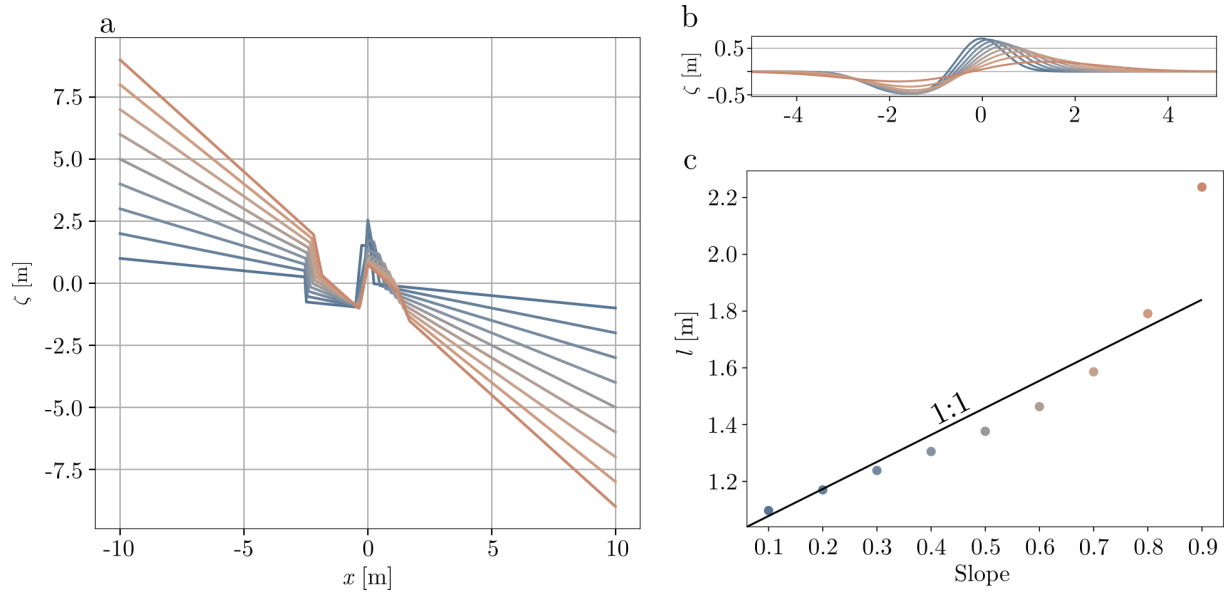
Figure S4. a) One dimensional model of an initial pit-mound couplet where a rectangle is uprooted perpendicular to the slope and all mass is dropped straight down on different slopes. On steeper slopes, more sediment falls downslope of the pit. b) Initial conditions of pit-mound couplets when we diffuse the profiles in (a) until a threshold slope is met - which is 1 in this case. c) Length-scale of the idealized pit-mound couplet that best fits the initial conditions in (b).